Numerical Calculation of MHD Equilibria including Static Magnetic Islands in a Straight Heliotron Configuration by Means of a Field Line Tracing Method*)

Kinya SAITO[1)], Katsuji ICHIGUCHI[1,2)] and Ryuichi ISHIZAKI[1,2)]

[1)]*The Graduate University for Advanced Studies, Toki 509-5292, Japan*

[2)]*National Institute for Fusion Science, Toki 509-5292, Japan*

(Received 6 December 2011 / Accepted 4 March 2012)

Magnetohydrodynamics (MHD) equilibria including static magnetic islands for the reduced MHD equations in a straight heliotron plasma are calculated. The equilibria are obtained as the solution of the coupled equations of the constant pressure along each field line and the force balance. The former and the latter equations are solved by means of a field line tracing method and a relaxation method, respectively. There exist two kinds of solutions. One is the equilibrium of which the pressure profile is flat at the O-point and steep at the X-point. In this case, the pressure gradient is discontinuous at the separatrix of the magnetic island. The other is the equilibrium of which the pressure profile is flat at not only the O-point but also the X-point. In the case, the pressure gradient is continuous at the separatrix.

Keywords: heliotron, MHD equilibrium, static magnetic island, field line tracing, separatrix

DOI: 10.1585/pfr.7.2403032

1. Introduction

Magnetic islands induced by resonant magnetic perturbations (RMP) are extensively studied in magnetically confined fusion devices these days. Recent experimental and theoretical works on magnetic islands are summarized in Ref. [1]. In tokamaks, a lot of efforts are paid for the control of the edge localized mode with the island generation by the application of the RMP. In heliotrons, the growth and the decay of the static magnetic islands at finite beta are studied in the Large Helical Device (LHD) as well. In the present work, we focus on the static magnetic island in the LHD configuration. In the LHD configuration, there exists a magnetic hill in the plasma column. Therefore, resistive interchange modes can be destabilized easily. Ichiguchi et al. [2, 3] and Ishizawa et al. [4] showed magnetic islands are also generated by the nonlinear evolution of the interchange modes. These studies indicate that the magnetic islands induced by the RMP can interact with the interchange modes.

We have studied the interaction between the static magnetic islands generated by the RMP and the resistive interchange modes by using the reduced magnetohydrodynamics (MHD) equations [5] in straight heliotron plasmas. In the previous work, a profile corresponding to nested magnetic surfaces was employed for the equilibrium pressure. In this case, interchange modes grow as in the case without the islands. The island width is changed by the nonlinear saturation of the interchange modes [6, 7].

On the other hand, the equilibrium pressure profile consistent with the topology of the static islands is generally deformed so as to have local flat structure at the island region. The local flat structure is expected to affect the growth of the interchange mode. For the study of the deformation effect on the stability, equilibrium with the pressure profile consistent with the static islands is needed. We have obtained one of such MHD equilibria by utilizing a diffusion equation parallel to the field line for the equilibrium pressure calculation [8]. In this case, the resultant equilibrium pressure profile is flat at both the O-point and the X-point of the magnetic island. The equilibrium is useful for the study of the effect of the local annual flat structure of the pressure profile on the stability of the interchange mode, but not for the pressure profile which is steep at the X-point and flat at the O-point. Thus, we develop a numerical scheme to calculate equilibria with such pressure profile for the straight LHD configuration in this work.

2. Coupled Equations for Equilibrium

MHD equilibria including a static magnetic island with the mode number of $(m, n) = (1, 1)$ are studied, which correspond to the reduced MHD equations in a straight heliotron configuration. Here, m and n are the poloidal and toroidal mode numbers, respectively. The reduced MHD equations are suitable for the analysis of such low mode number physics, which are composed of the Ohm's law, the vorticity equation and the pressure equation for the

author's e-mail: saito.kinya@nifs.ac.jp

*) This article is based on the presentation at the 21st International Toki Conference (ITC21).

poloidal flux $\Psi(r,\theta,z)$, the stream function $\Phi(r,\theta,z)$ and the plasma pressure $P(r,\theta,z)$. The normalized equations in the cylindrical coordinates (r,θ,z) are given by

$$\frac{\partial\tilde{\Psi}}{\partial t} = -\boldsymbol{B}\cdot\nabla\tilde{\Phi} + \frac{1}{S}\tilde{J}_z, \tag{1}$$

$$\frac{\mathrm{d}\tilde{U}}{\mathrm{d}t} = -\boldsymbol{B}\cdot\nabla\tilde{J}_z + \frac{1}{2\epsilon^2}\nabla\Omega\times\nabla P\cdot\boldsymbol{z} + \nu\nabla_\perp^2\tilde{U} \tag{2}$$

and

$$\frac{\partial P}{\partial t} = (\boldsymbol{z}\times\nabla\tilde{\Phi})\cdot\nabla P + \kappa_\perp\nabla_\perp^2 P + \kappa_\parallel(\boldsymbol{B}\cdot\nabla)(\boldsymbol{B}\cdot\nabla)P. \tag{3}$$

Here, the magnetic field is expressed as

$$\boldsymbol{B}(r,\theta,z) = \boldsymbol{z} + \boldsymbol{z}\times\nabla\ \Psi(r,\theta,z), \tag{4}$$

where $\boldsymbol{z}$ denotes the unit vector in the z direction. In this study, $\Psi(r,\theta,z)$ is expressed as

$$\Psi(r,\theta,z) = \Psi_{\mathrm{sym}}(r) + \Psi^{\mathrm{ext}}_{m,n}(r,\theta,z) + \tilde{\Psi}(r,\theta,z). \tag{5}$$

Here, $\Psi_{\mathrm{sym}}(r)$, $\Psi^{\mathrm{ext}}_{m,n}(r,\theta,z)$ and $\tilde{\Psi}(r,\theta,z)$ are the symmetric part in the case without the static island, the external poloidal flux which generates static magnetic islands with mode number (m,n) and the change of the poloidal flux due to the imposition of the islands, respectively. As shown in Refs. [9–11], $\Psi^{\mathrm{ext}}_{m,n}(r,\theta,z) = \hat{\Psi}^{\mathrm{ext}}_{m,n}(r)\cos(m\theta - nz)$ is given as the solution of no-current condition,

$$\nabla_\perp^2\Psi^{\mathrm{ext}}_{m,n}(r,\theta,z) = 0 \tag{6}$$

under the boundary conditions of

$$\hat{\Psi}^{\mathrm{ext}}_{m,n}(0) = 0 \quad \text{and} \quad \hat{\Psi}^{\mathrm{ext}}_{m,n}(1) = \Psi_{\mathrm{b}}, \tag{7}$$

where "$\wedge$" means the Fourier coefficients. Here, Ψ_{b} is the value of the external poloidal flux at the plasma boundary. In the case with $(m,n) = (1,1)$, $\hat{\Psi}^{\mathrm{ext}}_{1,1}(r)$ is given by $\hat{\Psi}^{\mathrm{ext}}_{1,1}(r) = \Psi_{\mathrm{b}}r$. The current density in the z direction $\tilde{J}_z$ and the vorticity in the z direction $\tilde{U}$ are expressed as $\tilde{J}_z = \nabla_\perp^2\tilde{\Psi}$ and $\tilde{U} = \nabla_\perp^2\tilde{\Phi}$, respectively, where $\nabla_\perp^2$ is given by $\nabla_\perp^2 = (1/r)(\partial/\partial r)(r\partial/\partial r) + (1/r^2)(\partial^2/\partial\theta^2)$. The convective time derivative is given by

$$\frac{\mathrm{d}}{\mathrm{d}t} = \frac{\partial}{\partial t} + \nabla\tilde{\Phi}\times\boldsymbol{z}\cdot\nabla. \tag{8}$$

The quantity $\nabla\Omega$ denotes the averaged field line curvature and Ω is given by [12]

$$\Omega(r) = \frac{\epsilon^2 N_{\mathrm{t}}}{l}\left(r^2\iota_{\mathrm{sym}} + 2\int r\iota_{\mathrm{sym}}\mathrm{d}r\right), \tag{9}$$

where ϵ, N_{t} and l are the inverse aspect ratio, the toroidal period number and the pole number of the helical coils, respectively. Here, ι is the rotational transform defined as

$$\iota(r) = \iota_{\mathrm{sym}}(r) + \tilde{\iota}(r), \tag{10}$$

where ι_{sym} and $\tilde{\iota}$ are given by

$$\iota_{\mathrm{sym}}(r) = \frac{1}{r}\frac{\mathrm{d}\Psi_{\mathrm{sym}}(r)}{\mathrm{d}r} \quad \text{and} \quad \tilde{\iota}(r) = \frac{1}{r}\frac{\mathrm{d}<\tilde{\Psi}>(r)}{\mathrm{d}r} \tag{11}$$

where $<\tilde{\Psi}>$ denotes the average part of $\tilde{\Psi}$.

The quantities $(r, z, t, \Psi, \Phi, P, U, J_z, \nu, \kappa_\perp, \kappa_\parallel)$ are normalized by $(a,\ R_0,\ \tau_{\mathrm{A}},\ a^2B_0/R_0,\ a^2/\tau_{\mathrm{A}},\ B_0^2/2\mu_0,\ 1/\tau_{\mathrm{A}},\ B_0/\mu_0R_0,\ \rho a^2/\tau_{\mathrm{A}},\ a^2/\tau_{\mathrm{A}},\ R_0^2/\tau_{\mathrm{A}})$, respectively. Here, B_0, a, $2\pi R_0$ and μ_0 denote the magnetic field at the magnetic axis, the plasma radius, the periodic length in z direction and the vacuum permeability, respectively. The viscosity and the perpendicular and the parallel heat conductivities are introduced with the coefficients ν, $\kappa_\perp$ and $\kappa_\parallel$, respectively. The magnetic Reynold's number S is defined as $S = \tau_{\mathrm{R}}/\tau_{\mathrm{A}}$. Here, the Alfvén time τ_{A} and the resistive diffusion time τ_{R} are given by $\tau_{\mathrm{A}} = R_0\sqrt{\mu_0\rho}/B_0$, $\tau_{\mathrm{R}} = \mu_0a^2/\eta$, where ρ and η are the mass density and the resistivity, respectively.

The equilibrium corresponding to Eqs. (1)-(3) with static islands needs to satisfy the following two equations. One is the constraint that the pressure is constant along field line with arbitrary topology,

$$\boldsymbol{B}\cdot\nabla P = 0, \tag{12}$$

which is obtained by assuming $\partial/\partial t = 0$, $\Phi = 0$ and $\kappa_\parallel \gg \kappa_\perp$ in Eq. (3). The other is the force balance equation given by

$$-\boldsymbol{B}\cdot\nabla\tilde{J}_z + \frac{1}{2\epsilon^2}\nabla\Omega\times\nabla P\cdot\boldsymbol{z} = 0 \tag{13}$$

which is obtained by $\partial/\partial t = 0$ and $\Phi = 0$ in Eq. (2). Equations (12) and (13) are coupled equations for $\Psi(r,\theta,z)$ and $P(r,\theta,z)$.

3. Two-Step Calculation Method

We solve Eqs. (12) and (13) in two separate steps like the schemes shown in Refs. [13–15]. In the first step, Eq. (12) is solved for P with Ψ fixed. A field line tracing method is employed in this step. We trace a field line from the initial point of (r_0, θ_0, z_0) and set the pressure as $P(r,\theta,z) = P_{\mathrm{sym}}(r_0)$ along the field line to make the pressure constant. Here, $P_{\mathrm{sym}}(r)$ is the pressure profile corresponding to the nested magnetic surfaces without magnetic islands. We fix θ_0 as $\theta_0 = \theta_{\mathrm{X}}$ which is the azimuthal angle of the position of the X-point for given z_0. By changing r_0, we can trace every field line outside the separatrix. The pressure inside the separatrix of the island is set to the value at the X-point.

In the second step, Eq. (13) is solved for Ψ with P fixed. The second step is a relaxation process given by Eq. (1) and the equation of

$$\frac{\partial\tilde{U}}{\partial t} = -\boldsymbol{B}\cdot\nabla\tilde{J}_z + \frac{1}{2\epsilon^2}\nabla\Omega\times\nabla P\cdot\boldsymbol{z} + \nu\nabla_\perp^2\tilde{U}. \tag{14}$$

To accelerate the relaxation process, we drop the convection term in Eq. (14). We regard the steady state as the equilibrium state as in Ref. [13]. In order to judge the achievement of the steady state, we observe the growth rates of the kinetic energy E_K and the magnetic energy E_M given by

$$\gamma_\mathrm{K} = \frac{1}{E_\mathrm{K}}\frac{\mathrm{d}E_\mathrm{K}}{\mathrm{d}t} \quad \text{and} \quad \gamma_\mathrm{M} = \frac{1}{E_\mathrm{M}}\frac{\mathrm{d}E_\mathrm{M}}{\mathrm{d}t}, \tag{15}$$

respectively, where

$$E_\mathrm{K} = \frac{1}{2}\int |\nabla\tilde{\Phi}\times z|^2 \mathrm{d}V \quad \text{and}$$
$$E_\mathrm{M} = \frac{1}{2}\int |z\times\nabla\tilde{\Psi}|^2 \mathrm{d}V. \tag{16}$$

When the conditions of

$$|\gamma_\mathrm{K}| < \epsilon_\gamma \quad \text{and} \quad |\gamma_M| < \epsilon_\gamma, \tag{17}$$

are satisfied simultaneously, we judge that the steady state is achieved. Since we introduce a small value of $1/S$ for the numerical stability in Eq. (1) of this step, we also check the force balance condition of Eq. (13) by evaluating ΔF_i defined as

$$\Delta F_i = \frac{|F_B + F_P|}{|F_B| + |F_P|}, \tag{18}$$

where the subscript i denotes the number of iteration. Here F_B and F_P are given by

$$F_B = \int(-\boldsymbol{B}\cdot\nabla\tilde{J}_z)\mathrm{d}V \quad \text{and}$$
$$F_P = \int\left(\frac{1}{2\epsilon^2}\nabla\Omega\times\nabla P\cdot z\right)\mathrm{d}V, \tag{19}$$

respectively.

The two steps described above are iterated until the island width w_i is converged, which is normalized by a. When the change rate δw_i of w_i satisfies the condition,

$$|\delta w_i| < \epsilon_w, \tag{20}$$

we judge that the MHD equilibrium is obtained, where δw_i is defined as

$$\delta w_i = \frac{w_i - w_{i-1}}{w_{i-1}}. \tag{21}$$

4. Results

By means of the two-step method explained in Sec. 3, MHD equilibria including static magnetic islands are obtained in a straight heliotron plasma. We employ the magnetic configuration parameters of $N_\mathrm{t} = 10$, $l = 2$ and $\epsilon = 0.16$, which correspond to the LHD configuration. We vary the value of Ψ_b from 0 to 1.0×10^{-3} in this study. In the case of positive Ψ_b, the X-point is located at $\theta_\mathrm{X} = 0$ and $z = 0$. Hence, we set $\theta_0 = 0$ and $z_0 = 0$ in the first step. The pressure profile $P_\mathrm{sym}(r)$,

$$P_\mathrm{sym}(r) = \beta_0(1 - r^4)^2 \tag{22}$$

is used with $\beta_0 = 1.5\%$. Since we use $P_\mathrm{sym}(r)$ of Eq. (22) as the pressure at the initial point (r_0, θ_0, z_0) at each iteration, the profile at (r, θ_0, z_0) for any r, and therefore, the gradient at the X-point is fixed over the whole iterations. In the second step, dissipation parameters are set to be $S = 10^2$ and $\nu = 10^{-6}$. We employ $\epsilon_\gamma = 10^{-6}$ and $\epsilon_w = 10^{-4}$ as the convergence parameters.

Figure 1 shows the resultant equilibrium pressure for $\Psi_\mathrm{b} = 1.0\times10^{-3}$. We obtain an equilibrium pressure profile which is steep at the X-point and flat at the O-point with the present scheme. Figure 2 shows the changes of

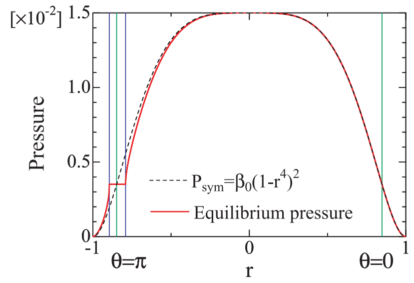

Fig. 1 Equilibrium pressure profile along the line connecting $(r = 1, \theta = 0, z = 0)$ and $(r = 1, \theta = \pi, z = 0)$ for $\Psi_\mathrm{b} = 1.0\times10^{-3}$ and $\beta_0 = 1.5\%$. Blue lines indicate the position of the separatrix of the island at $\theta = \pi$. Green lines indicate the position of the rational surface.

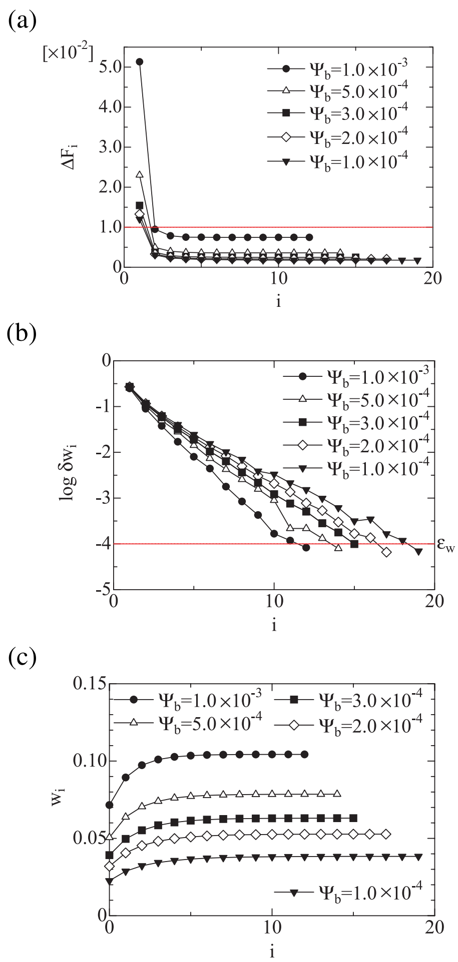

Fig. 2 Variation of (a) ΔF_i, (b) δw_i and (c) w_i.

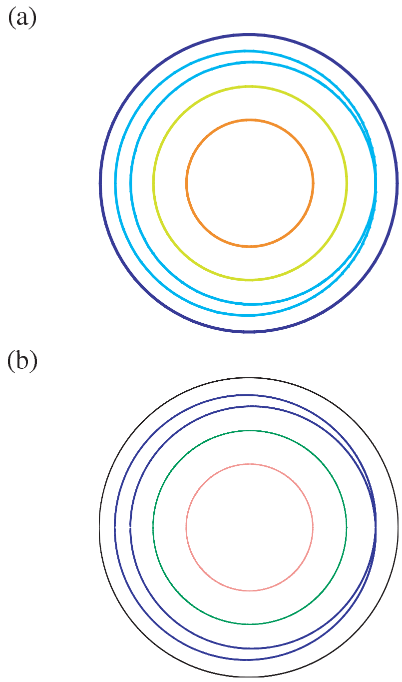

Fig. 3 Plots of (a) contour of constant pressure and (b) magnetic surfaces for $\Psi_b = 10^{-3}$ and $\beta_0 = 1.5\%$.

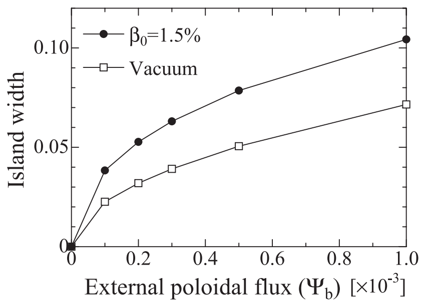

Fig. 4 Dependence of equilibrium island width on Ψ_b.

ΔF_i, δw_i and w_i in the iterations for several Ψ_b's. In the final states, $\Delta F_i < 10^{-2}$ is satisfied as shown in Fig. 2 (a), which indicates that the equilibrium is obtained in a good accuracy. Figure 2 (b) shows that the island width is converged in the finite number of iteration for every Ψ_b. The converged equilibrium island width is larger than the vacuum width w_0 as shown in Fig. 2 (c). The contour of the constant pressure coincides with the magnetic surfaces as shown in Fig. 3. That is, the equilibrium pressure has the same structure as that of the island. Figure 4 shows the dependence of the island width on Ψ_b. The island width is increased by the finite beta. The increment is increased with Ψ_b.

5. Discussions

In this work, the obtained equilibrium pressure profile is steep at the X-point and flat at the O-point as shown in Fig. 1. On the other hand, in the previous work [8], the

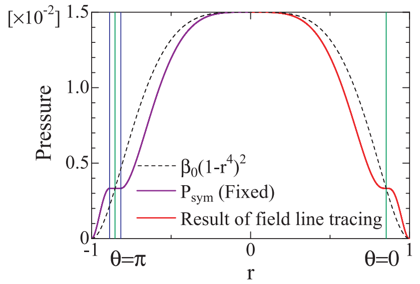

Fig. 5 Pressure profiles along the line connecting $(r = 1, \theta = 0, z = 0)$ and $(r = 1, \theta = \pi, z = 0)$ for $\Psi_b = 1.0 \times 10^{-3}$ and $\beta_0 = 1.5\%$. Purple and red lines show the assumed profile of $P(r_0, \theta_0 = \pi, z_0 = 0)$ with continuous gradient at the separatrix and the profile obtained by the tracing field lines starting from $(r_0, \theta_0 = \pi, z_0 = 0)$, respectively. Blue lines indicate the position of separatrix of island at $\theta = \pi$. Green lines indicate the position of the rational surface.

equilibrium pressure profile which is flat at not only the O-point but also the X-point is obtained. The difference in the pressure gradient at the X-point is attributed to the continuity of the pressure gradient across the separatrix except the X-point. In this work, the pressure gradient is discontinuous across the separatrix as shown in Fig. 1 because we employ the field line tracing method explained in Sec. 3. This discontinuity is inevitable for the existence of the finite gradient at the X-point. In the previous work [8], in order to satisfy Eq. (12), we calculate the steady state of the diffusion equation parallel to the field line,

$$\frac{\partial P}{\partial t} = \kappa_{\parallel}(\boldsymbol{B}\cdot\nabla)(\boldsymbol{B}\cdot\nabla)P. \tag{23}$$

In the right hand side of Eq. (23), the derivatives in r and θ directions are included. The continuity of the derivatives are naturally guaranteed in the numerical calculation. Therefore, the pressure gradient is continuous even at the separatrix [8]. This continuity makes the profile at the X-point flat.

This situation can be confirmed also with the present field line tracing scheme. We start the field line tracing from the initial point of $(r_0, \theta_0 = \pi, z_0 = 0)$ instead of $(r_0, \theta_0 = 0, z_0 = 0)$ used in the calculation for the pressure profile with steep gradient at the X-point. We assume $P_{\mathrm{sym}}(r)$ which is plotted with the purple solid line in the region of $-1 \le r \le 0$ at $\theta = \pi$ in Fig. 5 instead of Eq. (22). The gradient of this profile is continuous at the separatrix. Then, we obtain the profile plotted with the red solid line in the region of $0 \le r \le 1$ at $\theta = 0$ in Fig. 5 as the result of the field line tracing method. This result shows that the gradient at the X-point is necessary zero for the continuous gradient at the separatrix. This result also means that the present field line tracing method can generate the equilibrium solutions with which the pressure profile is flat at the X-point as well. Actually, the result obtained in Ref. [8] is directly confirmed with this method.

6. Conclusions

A numerical scheme to calculate MHD equilibria including static magnetic islands for the reduced MHD equations in a straight heliotron plasma is developed. The scheme is composed of the two steps solving the pressure and the poloidal flux. The original point of the scheme is in the field line tracing method in the pressure calculation. We calculate the pressure along a field line by replacing with a fixed value at a given azimuthal angle. By setting the azimuthal angle as that including the X-point, θ_X, we obtain an equilibrium with a finite pressure gradient at the X-point. The resultant equilibrium shows that the island width is increased by the finite beta value.

It is also found that there exist another kind of solution with a locally flat pressure profile at the X-point. Thus, there exist two kinds of equilibrium solutions depending on the gradient at the X-point, finite or zero. The difference of the equilibria is related to the continuity of the pressure gradient at the separatrix of the island except the X-point. The gradient at the X-point can be finite in the case where a discontinuous pressure gradient is allowed, while the gradient at the X-point must be zero in the case where only a continuous pressure gradient is allowed. In the former case, the solution is determined uniquely if the radial pressure profile at $\theta = \theta_X$ is specified. Since the pressure gradient is discontinuous at the separatrix, the second derivative of the radial pressure profile is infinite. On the other hand, in the latter case, the second derivative is finite. By rounding the radial pressure profile at the separatrix in the former solution or giving a finite second derivative to the former profile, we can obtain the latter solution. In this case, there exist various solutions depending on the shape of the roundness or the value of the second derivative. Therefore, the former solution can be considered as a special case of the latter case and the two solutions may be considered as a bifurcation. In both cases, it is assumed that the pressure is flat inside the separatrix in the present scheme. If a pressure profile corresponding to the magnetic surfaces inside the separatrix is incorporated, the freedom of the solution is increased.

It is interesting to obtain an equilibrium with a stochastic magnetic field by multi-helicity islands. However, the scheme developed here cannot be applied to the calculation of the equilibrium including a stochastic region. In the scheme, we fix a radial pressure profile at a given azimuthal position so that the solution should have the profile at the position. This treatment is possible only for the cases with radially separated islands. In the stochastic case, it is impossible to predict the pressure profile to be fixed at any azimuthal position before the calculation.

The obtained result in the present work is utilized in the stability analysis of the interchange mode in the equilibria with the magnetic islands. It is already known that annular flat structure around the resonant surface in the pressure profile has a stabilizing contribution on the interchange mode [16]. The resultant equilibria in the present work have a steep pressure gradient at the X-point. Thus, it is expected that the stabilizing contribution is smaller than that in the annular flat structure case. The quantitative results of the linear stability and the nonlinear evolution will be discussed in another paper [17].

Acknowledgments

One of authors (K. S.) would like to thank Dr. Y. Suzuki and Dr. R. Kanno for helpful discussions and lots of suggestions. This work is partly supported by budget NIFS11KNXN222 of National Institute for Fusion Science and by the Grant-in-Aid for Scientific Research (C) 22560822 from JSPS, Japan.

[1] F.L. Waelbroeck, Nucl. Fusion **49**, 104025 (2009).
[2] K. Ichiguchi *et al.*, Nucl. Fusion **43**, 1101 (2003).
[3] K. Ichiguchi and B.A. Carreras, J. Plasma Fusion Res. SERIES **6**, 589 (2004).
[4] A. Ishizawa and N. Nakajima, Phys. Plasmas **17**, 072308 (2010).
[5] H. R. Strauss, Plasma Phys. **22**, 733 (1980).
[6] K. Saito *et al.*, Phys. Plasmas **17**, 062504 (2010).
[7] K. Saito *et al.*, Plasma Fusion Res. **6**, 02403072 (2011).
[8] K. Saito *et al.*, submitted to Plasma Fusion Res.
[9] T. Unemura *et al.*, Phys. Plasmas **11**, 1545 (2004).
[10] L. Garcia *et al.*, Phys. Plasmas **8**, 4111 (2001).
[11] L. Garcia *et al.*, Nucl. Fusion **43**, 553 (2003).
[12] M. Wakatani, *Stellarator and Heliotron Devices* (Oxford University Press, New York, 1998), p.98.
[13] W. Park *et al.*, Phys. Fluids **29** (4), 1171 (1986).
[14] K. Harafuji *et al.*, J. Comput. Phys. **81**, 169 (1989).
[15] Y. Suzuki *et al.*, Nucl. Fusion **46**, L19 (2006).
[16] K. Ichiguchi *et al.*, Nucl. Fusion **41**, 181 (2001).
[17] K. Saito *et al.*, to be submitted to Plasma Fusion Res.